

Phasing out Dark Matter Isocurvature with Thermal Misalignment

Brian Batell,^{1,*} Akshay Ghalsasi,^{1,2,†} Subhajit Ghosh,^{3,‡} and Mudit Rai^{1,4,§}

¹*Pittsburgh Particle Physics, Astrophysics, and Cosmology Center,*

Department of Physics and Astronomy, University of Pittsburgh, Pittsburgh, USA

²*Jefferson Physical Laboratory, Harvard University, Cambridge, MA 02138, USA*

³*Texas Center for Cosmology and Astroparticle Physics, Weinberg Institute,
Department of Physics, The University of Texas at Austin, Austin, TX 78712, USA*

⁴*Mitchell Institute for Fundamental Physics and Astronomy,
Department of Physics and Astronomy, Texas A&M University, College Station, USA*

(Dated: March 20, 2026)

Abstract

Thermal misalignment provides an alternative to the standard misalignment mechanism for the cosmological production of scalar dark matter. In this framework, feeble couplings to particles in the thermal bath generate a finite-temperature potential that drives the scalar towards large field values early in the radiation era, dynamically inducing the misalignment before the onset of scalar oscillations. As a result, the relic abundance is controlled primarily by particle masses and couplings rather than the initial field value. As a light spectator field, the scalar acquires inflationary fluctuations that are uncorrelated with the adiabatic curvature mode, generically sourcing isocurvature perturbations. We show that, unlike standard misalignment, where light scalars are strongly constrained by cosmic microwave background bounds on dark matter isocurvature for high-scale inflation, thermal misalignment can naturally suppress the isocurvature signal. This occurs through a novel late-time phase offset between the background zero mode and the super-horizon perturbations, which reduces the final dark matter density contrast. Thermal misalignment therefore provides a new and generic route to isocurvature-safe scalar dark matter.

* batell@pitt.edu

† aghalsasi@fas.harvard.edu

‡ sghosh@utexas.edu

§ muditrai@tamu.edu

I. INTRODUCTION

Deciphering the nature of dark matter (DM), which accounts for about a quarter of the energy budget of the Universe [1], remains one of the central goals of particle physics and cosmology. While the existence of DM is well established through a broad array of astrophysical and cosmological observations, its microscopic identity remains obscure, from its basic dynamical properties to the origin of its cosmic abundance.

An appealing DM candidate is an ultralight scalar field ϕ with very weak couplings to other fields. The scalar relic abundance is generically generated by the misalignment mechanism [2–4]: the field is initially displaced from its minimum, is frozen by Hubble friction in the early radiation era, and begins coherent oscillations when the Hubble rate falls below its mass. The oscillating condensate redshifts as non-relativistic matter and therefore acts as cold DM. In the standard misalignment scenario, the scalar relic abundance is determined by its initial displacement ϕ_i and does not depend on its couplings to other particles in the thermal bath. Popular realizations of this scenario include the QCD axion, axion-like particles, as well as dilatons and other light scalar fields (see Ref. [5] for a comprehensive review).

In this work we study the thermal misalignment mechanism [6–8], an alternative to the standard misalignment mechanism for the cosmological production of the ultralight scalar DM. In this framework, the scalar couples feebly to states in the thermal bath through couplings that break its shift symmetry. The resulting finite-temperature correction to the effective potential in the early radiation era pushes the field toward its high-temperature minimum at large field values, thereby generating the misalignment dynamically. If the initial field value is small compared to the thermally induced misalignment, the late-time oscillation amplitude and resulting relic abundance becomes insensitive to initial conditions and is instead set by the particle masses and scalar couplings to particles in the bath. Thermal misalignment therefore yields a sharp prediction for the model parameters that reproduce the observed relic density. Thermal misalignment has been further studied in several scenarios with scalar DM coupled to SM particles [9–15], and the general phenomenon has also been explored in other contexts [16–22].

A key issue that has not yet been studied in the thermal misalignment scenario is the generation of isocurvature perturbations and their associated constraints. In the standard

misalignment scenario, ultralight scalar DM behaves as a spectator field during inflation and acquires quantum fluctuations uncorrelated with the adiabatic curvature perturbation generated by the inflaton. These fluctuations source DM isocurvature perturbations, which can leave observable imprints on the CMB anisotropies [23–35]. For a light field in quasi-de Sitter inflation, the fluctuation amplitude is $\delta\phi_i \sim H_I/(2\pi)$. Since the relic abundance from standard misalignment scales as $\rho_\phi \propto m_\phi^2 \phi_i^2$ with m_ϕ the scalar mass, inflationary fluctuations induce isocurvature of order $\delta\rho_\phi/\rho_\phi \sim 2\delta\phi_i/\phi_i \sim H_I/\pi\phi_i$. CMB observations, including Planck [36], have uncovered no evidence for primordial isocurvature and therefore place an upper bound on the inflationary Hubble scale $H_I \leq 1.7 \times 10^7 \text{ GeV} \times (m_\phi/\text{eV})^{-1/4}$. Reproducing the observed amplitude of primordial curvature perturbations with simple, natural inflationary potentials often points to a relatively high inflation scale, well above the bound discussed above, though still subject to the CMB constraint of $H_I \lesssim 4.7 \times 10^{13} \text{ GeV}$ from the non-observation of primordial tensor modes [37]. Moreover, although low-scale inflation remains viable, many well-studied low-scale constructions are small-field models, which are often less robust to inhomogeneous initial conditions than large-field models [38]. This tension between high-scale inflation and light scalar DM, as implied by CMB isocurvature bounds, has been emphasized repeatedly in the literature, particularly for axions [23, 25, 27–29, 39–42]. Several classes of solutions have been proposed for axion DM, including mechanisms that rely on making the axion heavy during inflation to suppress the amplitude of isocurvature perturbations [43–59] or that reduce the axion decay constant following inflation [60–73] (see [43] for more discussion).

Since thermal misalignment alters the post-inflationary evolution of the scalar field, it is natural to ask whether the same isocurvature constraints apply in that scenario. Our main goal in this work is to study the evolution of isocurvature perturbations in the thermal misalignment scenario and the resulting constraints on parameter space. To this end, we focus on the simple representative model studied in Ref. [7], consisting of an ultralight scalar DM field coupled to a fermion that is in thermal equilibrium with the SM plasma. We find that, compared to standard misalignment, the isocurvature can be dynamically suppressed in regions of parameter space where the scalar starts oscillating before the thermal potential has switched off. Intuitively, standard misalignment corresponds to a field released from rest, while thermal misalignment can release the field with a sizable initial velocity. This produces an approximately $-\pi/2$ phase shift in the late-time zero mode oscillation, leading to

a relative phase offset with the superhorizon perturbation and thus a suppressed DM density contrast. This provides a novel mechanism for suppressing DM isocurvature, distinct from the existing approaches in the axion literature (see previous paragraph), which instead rely on suppressing the amplitude of the primordial isocurvature perturbations.

The remainder of the paper is organized as follows. In Section II, we introduce the model with a scalar–fermion Yukawa coupling and outline the basic setup for the evolution equations governing the background and superhorizon perturbations in the perturbed expanding universe. In Section III, we develop the solution for the late-time evolution of the scalar zero mode and relate the scalar–fermion coupling to the present-day DM abundance. In Section IV, we solve for the late-time behavior of the superhorizon perturbations. In Section V, we combine these results to determine the modification of large-scale isocurvature in thermal misalignment. We then discuss the implications in Section VI, where we show that DM isocurvature can be suppressed. Finally, we conclude and provide an outlook in Section VII.

II. THERMAL MISALIGNMENT: MODEL AND SETUP

We are interested in the production of DM via the thermal misalignment mechanism and the accompanying generation of isocurvature perturbations. To this end, we work in a perturbed Friedmann–Robertson–Walker (FRW) spacetime and adopt the Newtonian gauge. The metric takes the form [74–77]

$$ds^2 = -[1 + 2\Psi(t, \mathbf{x})]dt^2 + a^2(t)[1 + 2\Phi(t, \mathbf{x})]\delta_{ij}dx^i dx^j, \quad (1)$$

where $a(t)$ is the scale factor and Ψ, Φ are the scalar metric perturbations.

Throughout this work, we focus on a prototypical model consisting of a real scalar field ϕ , which serves as the DM candidate, coupled feebly to a Dirac fermion ψ via a Yukawa interaction. The Lagrangian is given by

$$-\mathcal{L} \supset \frac{1}{2}m_\phi^2\phi^2 + m_\psi \left(1 - \frac{\beta\phi}{M_{\text{pl}}}\right) \bar{\psi}\psi, \quad (2)$$

where m_ϕ (m_ψ) denotes the scalar (fermion) mass, $M_{\text{pl}} = 2.4 \times 10^{18}$ GeV is the reduced Planck mass, and the Yukawa coupling is parameterized as $-\beta m_\psi/M_{\text{pl}}$ with β a real dimensionless parameter.

We assume the fermion ψ is in thermal equilibrium with the Standard Model (SM) plasma during the radiation era. The scalar field thus evolves under the influence of an effective potential $V(\phi, T)$, which includes the tree-level mass term in Eq. (2), $V_0(\phi) = \frac{1}{2}m_\phi^2\phi^2$, along with a finite-temperature correction arising from the thermal free energy density of ψ ,

$$\delta V(\phi, T) = -\frac{g_\psi}{2\pi^2}T^4 J_F \left[\frac{m_\psi^2(\phi)}{T^2} \right], \quad (3)$$

where $g_\psi = 4$ accounts for the fermion spin degrees of freedom, $m_\psi(\phi) = m_\psi(1 - \beta\phi/M_{\text{pl}})$ is the effective fermion mass in the scalar background, and

$$J_F(w^2) = \int_0^\infty dx x^2 \log \left[1 + e^{-\sqrt{x^2+w^2}} \right], \quad (4)$$

with $w^2 = (m_\psi^2/T^2)(1 - \beta\phi_0/M_{\text{pl}})^2$.

Aside from its coupling to ψ in Eq. (2), we assume ϕ has negligible couplings to other particles in the thermal bath. Thus, although ψ is in thermal equilibrium, ϕ never thermalizes, and thermal freeze-in produces a negligible scalar relic abundance, owing to the extremely suppressed scalar–fermion coupling.

We decompose the scalar field into a spatially homogeneous, time-dependent background $\phi_0(t)$ and a perturbation $\phi_1(t, \mathbf{x})$,

$$\phi(t, \mathbf{x}) = \phi_0(t) + \phi_1(t, \mathbf{x}). \quad (5)$$

The SM bath temperature is also perturbed according to $T(t, \mathbf{x}) \rightarrow T(t) + \delta T(t, \mathbf{x})$. Expanding the equations of motion to linear order in perturbations yields the evolution equations for ϕ_0 and ϕ_1 . For the perturbations, we track the evolution of the Fourier modes, e.g., $\phi_1(t, \mathbf{k})$ defined via

$$\phi_1(t, \mathbf{x}) = \int \frac{d^3k}{(2\pi)^3} e^{i\mathbf{k}\cdot\mathbf{x}} \phi_1(t, \mathbf{k}). \quad (6)$$

The equations governing $\phi_0(t)$ and $\phi_1(t, \mathbf{k})$ are (overdots denote derivatives with respect to coordinate time t)

$$\ddot{\phi}_0 + 3H\dot{\phi}_0 + V_\phi = 0, \quad (7)$$

$$\ddot{\phi}_1 + 3H\dot{\phi}_1 + \left(\frac{k^2}{a^2} + V_{\phi\phi} \right) \phi_1 + (-\dot{\Psi} + 3\dot{\Phi})\dot{\phi}_0 + 2\Psi V_\phi + V_{\phi T}\delta T = 0, \quad (8)$$

where $H = \dot{a}/a$ is the Hubble parameter, $V_\phi \equiv \partial V/\partial\phi$, $V_{\phi\phi} \equiv \partial^2 V/\partial\phi^2$, and $V_{\phi T} \equiv$

$\partial^2 V / \partial \phi \partial T$. The various derivatives appearing in the evolution equations are given by

$$V_\phi = m_\phi^2 \phi_0 + \frac{g_\psi \beta m_\psi^2 T^2}{\pi^2 M_{\text{pl}}} \left(1 - \frac{\beta \phi_0}{M_{\text{pl}}} \right) J'_F(w^2), \quad (9)$$

$$V_{\phi\phi} = m_\phi^2 - \frac{g_\psi \beta^2 m_\psi^2 T^2}{\pi^2 M_{\text{pl}}^2} [J'_F(w^2) + 2w^2 J''_F(w^2)], \quad (10)$$

$$V_{\phi T} = \frac{2g_\psi \beta m_\psi^2 T}{\pi^2 M_{\text{pl}}} \left(1 - \frac{\beta \phi_0}{M_{\text{pl}}} \right) [J'_F(w^2) - w^2 J''_F(w^2)], \quad (11)$$

At late times, the scalar field energy density is decomposed into a background component and a perturbation:

$$\rho_\phi = \frac{1}{2} \dot{\phi}_0^2 + \frac{1}{2} m_\phi^2 \phi_0^2, \quad (12)$$

$$\delta\rho_\phi = \dot{\phi}_0 \dot{\phi}_1 - \Psi \dot{\phi}_0^2 + m_\phi^2 \phi_0 \phi_1. \quad (13)$$

These will be used in the computation of the DM relic abundance and isocurvature perturbations.

We will be interested in the evolution of superhorizon modes, $k \ll aH$, during the radiation domination era, during which $H = 1/(2t) = \gamma T^2/M_{\text{pl}}$ with $\gamma(T) = \sqrt{\pi^2 g_*(T)/90}$ and $g_{*(S)}(T)$ the effective number of relativistic (entropy) degrees of freedom. We therefore neglect the k^2 term in Eq. (8), take $\Phi \approx -\Psi$ to be constant, $\dot{\Psi} = \dot{\Phi} \approx 0$, and $\delta T/T \approx -\Psi/2$. These approximations are valid during radiation domination in the absence of significant anisotropic stress and non-adiabatic pressure perturbation¹ [74–78]. It is also convenient to introduce the following dimensionless variables,

$$\varphi = \frac{\phi}{M_{\text{pl}}}, \quad x = m_\phi t, \quad \kappa = \frac{m_\phi M_{\text{pl}}}{m_\psi^2}, \quad x_\psi = \frac{m_\psi}{H(T = m_\psi)} = \frac{\kappa}{2\gamma}. \quad (14)$$

Here, φ is the field value relative to M_{pl} , x is the dimensionless time variable, while x_ψ corresponds to the “time” at which the temperature is equal to the fermion mass, $T = m_\psi$. The latter is proportional to the dimensionless combination of mass parameters κ . The evolution equations for the background and superhorizon perturbations in radiation

¹ Although, ϕ can induce non-adiabatic pressure perturbation [78], we neglect those effects in total curvature perturbation since ϕ carry a very small energy density compared to the radiation bath. This is consistent with our treatment of $H = 1/(2t)$ where we have only kept the radiation contribution.

domination, as well as the corresponding energy density equations, become

$$\frac{d^2\varphi_0}{dx^2} + \frac{3}{2x} \frac{d\varphi_0}{dx} + \mathcal{V}_\varphi = 0, \quad (15)$$

$$\frac{d^2\varphi_1}{dx^2} + \frac{3}{2x} \frac{d\varphi_1}{dx} + \mathcal{V}_{\varphi\varphi}\varphi_1 + 2\Psi\mathcal{V}_\varphi + \Psi x\mathcal{V}_{\varphi x} = 0, \quad (16)$$

$$\rho_\phi = m_\phi^2 M_{\text{pl}}^2 \left[\frac{1}{2} \left(\frac{d\varphi_0}{dx} \right)^2 + \frac{1}{2} \varphi_0^2 \right], \quad (17)$$

$$\delta\rho_\phi = m_\phi^2 M_{\text{pl}}^2 \left[\frac{d\varphi_0}{dx} \frac{d\varphi_1}{dx} - \Psi \left(\frac{d\varphi_0}{dx} \right)^2 + \varphi_0\varphi_1 \right], \quad (18)$$

where we have defined the dimensionless effective potential,

$$\begin{aligned} \mathcal{V}(\varphi, x) &\equiv \frac{V(\phi = M_{\text{pl}}\varphi, T = m_\psi\sqrt{x_\psi/x})}{m_\phi^2 M_{\text{pl}}^2} \\ &= \frac{1}{2}\varphi^2 - \frac{g_\psi}{2\pi^2} \frac{1}{\kappa^2} \frac{x_\psi^2}{x^2} J_F(w^2). \end{aligned} \quad (19)$$

where $w^2 = (x/x_\psi)(1 - \beta\varphi_0)^2$. Then, the various derivatives appearing in the evolution equations are given by

$$\mathcal{V}_\varphi = \varphi_0 + \frac{g_\psi}{\pi^2} \frac{\beta}{\kappa^2} \frac{x_\psi}{x} (1 - \beta\varphi_0) J'_F(w^2), \quad (20)$$

$$\mathcal{V}_{\varphi\varphi} = 1 - \frac{g_\psi}{\pi^2} \frac{\beta^2}{\kappa^2} \frac{x_\psi}{x} [J'_F(w^2) + 2w^2 J''_F(w^2)], \quad (21)$$

$$\mathcal{V}_{\varphi x} = -\frac{g_\psi}{\pi^2} \frac{\beta}{\kappa^2} \frac{x_\psi}{x^2} (1 - \beta\varphi_0) [J'_F(w^2) - w^2 J''_F(w^2)]. \quad (22)$$

In order to solve Eqs. (15,16), we must specify the initial conditions at time $x_i \simeq 2m_\phi/H_I \ll 1$ corresponding to the onset of the radiation era, where H_I is the inflationary Hubble scale and we have assumed instantaneous reheating. For the zero mode, assuming a minimal period of inflation with $N \sim 60$ e-folds, the comoving scale corresponding to our observable universe exits the horizon near the onset of inflation, so the background field value is simply set by the pre-inflationary initial condition, $\varphi_0(x_i) \equiv \varphi_{0i}$, which we treat as a free parameter, while the initial velocity is negligible, $d\varphi_0(x_i)/dx = 0$.² While in standard misalignment the relic abundance is set by a sizable initial field value φ_{0i} , the thermal misalignment regime is instead characterized by small initial field values in comparison to

² For a sufficiently long period of inflation, $N \gg H_I/m_\phi$, stochastic inflationary dynamics drives the scalar field to an equilibrium distribution with typical field value $\varphi_{0i} \sim H_I^2/m_\phi$ [71, 79, 80]. For small H_I , this can dynamically generate the small initial field values required for the thermal misalignment mechanism. However, since observationally significant isocurvature perturbations require a sufficiently large H_I we do not focus on this case here.

the eventual oscillation amplitude that is dynamically set in the early radiation era, so that in practice $\varphi_{0i} \simeq 0$.

The initial conditions for the superhorizon perturbations are set during inflation with the Bunch-Davies vacuum. Since $m_\phi \ll H_I$, in the de Sitter limit (neglecting slow-roll corrections) we have $|\varphi_1(x_i)| \equiv |\varphi_{1,i}| = H_I/(2M_{\text{pl}}k^{3/2})$ and $d\varphi_1(x_i)/dx = 0$, yielding the characteristic nearly scale invariant power spectrum for a light spectator field (see Section V below for further details).

It is worth remarking that, in addition to the finite-temperature correction in Eq. (3), the scalar effective potential also receives a zero-temperature one-loop contribution, namely the Coleman–Weinberg potential [81]. Throughout this work, we assume that the full zero-temperature effective potential is nevertheless well approximated by the simple quadratic form in Eq. (2). For small scalar masses m_ϕ and and sizable couplings β , this requires tuning of both the scalar mass term and the quartic coupling, reflecting the usual naturalness problem of light scalars. A rough criterion for radiative stability is $\beta \lesssim 4\pi\kappa$; see Fig. 2. In the regions where this condition is violated, fine-tuning of the scalar potential is required. Although we do not pursue this question here, it would be interesting to explore model-building mechanisms that protect such light, weakly coupled scalars; see Refs. [10, 82] for recent progress in this direction.

Our analysis adopts a phenomenological approach in which the scalar condensate evolves in a time-dependent effective potential. While this provides a leading description of thermal misalignment dynamics, it neglects potentially important nonequilibrium effects associated with the full real-time initial-value problem, including derivative terms in the effective action, particle production, and backreaction. Recent work has emphasized that, in Yukawa-coupled systems, these effects can qualitatively modify condensate evolution beyond what is captured by the effective potential alone [83]. While the finite-temperature, expanding background setting relevant for thermal misalignment differs from the zero-temperature Minkowski setup studied there, it would be interesting to investigate analogous nonequilibrium corrections in the present context. Relatedly, our analysis neglects possible thermal damping, a dissipative correction that can arise when the scalar background modulates the masses of particles in the thermal bath [84, 85]. As the scalar evolves, these species are driven slightly out of equilibrium, and their relaxation back to equilibrium induces an additional friction-like term beyond the leading thermal effective potential. We have checked that, for the couplings and

fermion masses relevant to our study, the associated damping rate is negligible and does not impact the scalar evolution or our results.

In the next two sections, we develop approximate analytic solutions to the evolution equations for the zero mode (15) and the superhorizon perturbations (16).

III. BACKGROUND EVOLUTION AND DARK MATTER ABUNDANCE

In this section we study the dynamical misalignment of the scalar background $\varphi_0(x)$ driven by the finite temperature effective potential and estimate the resulting DM relic abundance. We also determine the model parameters (coupling and masses) leading to the observed relic density. This section thus serves as a review of the thermal misalignment mechanism introduced in Ref. [7]. While our method for solving the zero-mode evolution differs from that used there, we recover the results.

To this end, we solve the evolution equation for $\varphi_0(x)$, Eqs. (16,20) with initial conditions $\varphi_0(x)|_{x_i} = \varphi_{0i}$, $d\varphi_0/dx|_{x_i} = 0$ at the beginning of the radiation era corresponding to $x = x_i \simeq 2m_\phi/H_I$. In practice, since $m_\phi \ll H_I$, we have $x_i \simeq 0$. As mentioned above, the thermal misalignment regime corresponds to small initial field values in comparison to the eventual oscillation amplitude. Nevertheless, we will retain $\varphi_{0i} \neq 0$ in constructing the zero mode solution for two reasons. First, this will allow us to recover the standard misalignment limit, $\beta \rightarrow 0$ with $\varphi_{0i} \neq 0$, allowing for a clear comparison with the thermal misalignment regime, $\beta \neq 0$ and $\varphi_{0i} \rightarrow 0$. Second, in the next section this more general solution will allow us to directly extract the evolution of the superhorizon perturbations.

As we will see shortly, for the vast majority of the viable parameter space, the correct relic abundance is obtained for couplings β and background field values φ_0 that satisfy the condition

$$\beta\varphi_0 \ll 1. \tag{23}$$

We use this fact to develop a semi-analytic solution to the evolution equation. To this end, we expand the derivative of the potential \mathcal{V}_φ (20) in the background evolution equation (15) to first order in $\beta\varphi_0$, leading to

$$\frac{d^2\varphi_0}{dx^2} + \frac{3}{2x} \frac{d\varphi_0}{dx} + \varphi_0 \simeq -\delta\tilde{\mathcal{V}}_\varphi(x) - \delta\tilde{\mathcal{V}}_{\varphi\varphi}\varphi_0, \tag{24}$$

where

$$\delta\tilde{\mathcal{V}}_\varphi(x) = \frac{g_\psi}{\pi^2} \frac{\beta}{\kappa^2} \frac{x_\psi}{x} J'_F(x/x_\psi), \quad (25)$$

$$\delta\tilde{\mathcal{V}}_{\varphi\varphi} = -\frac{g_\psi}{\pi^2} \frac{\beta^2}{\kappa^2} \frac{x_\psi}{x} [J'_F(x/x_\psi) + 2(x/x_\psi)J''_F(x/x_\psi)]. \quad (26)$$

The second term on the RHS of Eq. (24) represents a correction of order $\beta\varphi_0$ which we treat as a perturbation. We thus develop a perturbative solution for the background,

$$\varphi_0(x) \simeq \varphi_0^{(0)}(x) + \varphi_0^{(1)}(x). \quad (27)$$

We emphasize that $\varphi_0^{(1)}$ is **not** the inhomogeneous linear perturbation (i.e., φ_1), but is instead a first order correction to the homogeneous background in the $\beta\varphi_0 \ll 1$ limit. Plugging Eq. (27) into (24), we find that $\varphi_0^{(0)}$ and $\varphi_0^{(1)}$ evolve according to

$$\frac{d^2\varphi_0^{(0)}}{dx^2} + \frac{3}{2x} \frac{d\varphi_0^{(0)}}{dx} + \varphi_0^{(0)} = -\delta\tilde{\mathcal{V}}_\varphi, \quad (28)$$

$$\frac{d^2\varphi_0^{(1)}}{dx^2} + \frac{3}{2x} \frac{d\varphi_0^{(1)}}{dx} + \varphi_0^{(1)} = -\delta\tilde{\mathcal{V}}_{\varphi\varphi}\varphi_0^{(0)}, \quad (29)$$

This solution method corresponds to the Born approximation familiar from quantum mechanics. The terms on the right-hand side act as field-independent sources, while the homogeneous equations are readily solved in terms of Bessel functions. We therefore adopt a Green's function approach to solve Eqs. (28, 29).

The solution to Eq. (28), subject to the initial conditions at $x_i \simeq 0$ given by $\varphi_0^{(0)}(0) = \varphi_{0i}$, $d\varphi_0^{(0)}(0)/dx = 0$, is given by

$$\varphi_0^{(0)}(x) = \varphi_{0i} 2^{1/4} \Gamma(5/4) \frac{J_{1/4}(x)}{x^{1/4}} - \int_0^x dy \mathcal{G}(x, y) \delta\tilde{\mathcal{V}}_\varphi(y). \quad (30)$$

Here $\Gamma(z)$ is the Euler gamma function, while $\mathcal{G}(x, y)$ is the retarded Green's function, defined by $\mathcal{G}(x, y) = 0$ for $x < y$ and, for $x > y$,

$$\mathcal{G}(x, y) = \frac{\pi}{2} \frac{y^{5/4}}{x^{1/4}} [Y_{1/4}(x)J_{1/4}(y) - J_{1/4}(x)Y_{1/4}(y)], \quad (31)$$

with $J_{1/4}(x)$, $Y_{1/4}(x)$ the Bessel functions of order 1/4. The first (second) term in Eq. (30) represents the homogeneous (particular) solution.

Using Eq. (30) for $\varphi_0^{(0)}(x)$, we immediately obtain the solution to Eq. (29),

$$\varphi_0^{(1)}(x) = - \int_0^x dy \mathcal{G}(x, y) \delta\tilde{\mathcal{V}}_{\varphi\varphi}(y) \varphi_0^{(0)}(y). \quad (32)$$

The full solution to the background field equation, valid for small $\beta\varphi_0$, is given by the sum of (30) and (32) and may be written as

$$\varphi_0(x) = \mathcal{A}(x, x_\psi) \frac{J_{1/4}(x)}{x^{1/4}} + \mathcal{B}(x, x_\psi) \frac{Y_{1/4}(x)}{x^{1/4}}, \quad (33)$$

where the coefficients \mathcal{A} and \mathcal{B} are given by

$$\begin{aligned} \mathcal{A}(x, x_\psi) &= \varphi_{0i} 2^{1/4} \Gamma(5/4) + \frac{g_\psi}{4\gamma\pi} \frac{\beta}{\kappa} \mathcal{F}_Y(x, x_\psi) - \varphi_{0i} 2^{1/4} \Gamma(5/4) \frac{g_\psi}{2\pi} \frac{\beta^2}{\kappa^2} \mathcal{F}_{JY}(x, x_\psi) \\ &+ \frac{g_\psi^2}{8\gamma\pi^2} \frac{\beta^3}{\kappa^3} \left[\mathcal{F}_{YYJ}(x, x_\psi) - \mathcal{F}_{JYY}(x, x_\psi) \right], \end{aligned} \quad (34)$$

$$\begin{aligned} \mathcal{B}(x, x_\psi) &= -\frac{g_\psi}{4\gamma\pi} \frac{\beta}{\kappa} \mathcal{F}_J(x, x_\psi) + \varphi_{0i} 2^{1/4} \Gamma(5/4) \frac{g_\psi}{2\pi} \frac{\beta^2}{\kappa^2} \mathcal{F}_{JJ}(x, x_\psi) \\ &- \frac{g_\psi^2}{8\gamma\pi^2} \frac{\beta^3}{\kappa^3} \left[\mathcal{F}_{JYJ}(x, x_\psi) - \mathcal{F}_{JJY}(x, x_\psi) \right]. \end{aligned} \quad (35)$$

The coefficients depend on the integrals $\mathcal{F}_J, \mathcal{F}_Y, \mathcal{F}_{JJ}, \mathcal{F}_{JY}, \mathcal{F}_{JYJ}, \mathcal{F}_{JJY}, \mathcal{F}_{YYJ}, \mathcal{F}_{JYY}$, which are defined as

$$\mathcal{F}_J(x, x_\psi) = \int_0^x dy y^{1/4} J_{1/4}(y) J'_F(y/x_\psi), \quad (36)$$

$$\mathcal{F}_Y(x, x_\psi) = \int_0^x dy y^{1/4} Y_{1/4}(y) J'_F(y/x_\psi), \quad (37)$$

$$\mathcal{F}_{JJ}(x, x_\psi) = x_\psi \int_0^x dy [J'_F(y/x_\psi) + 2(y/x_\psi) J''_F(y/x_\psi)] J_{1/4}^2(y), \quad (38)$$

$$\mathcal{F}_{JY}(x, x_\psi) = x_\psi \int_0^x dy [J'_F(y/x_\psi) + 2(y/x_\psi) J''_F(y/x_\psi)] J_{1/4}(y) Y_{1/4}(y), \quad (39)$$

$$\mathcal{F}_{JYJ}(x, x_\psi) = x_\psi \int_0^x dy [J'_F(y/x_\psi) + 2(y/x_\psi) J''_F(y/x_\psi)] J_{1/4}(y) Y_{1/4}(y) \mathcal{F}_J(y, x_\psi), \quad (40)$$

$$\mathcal{F}_{JJY}(x, x_\psi) = x_\psi \int_0^x dy [J'_F(y/x_\psi) + 2(y/x_\psi) J''_F(y/x_\psi)] J_{1/4}^2(y) \mathcal{F}_Y(y, x_\psi), \quad (41)$$

$$\mathcal{F}_{YYJ}(x, x_\psi) = x_\psi \int_0^x dy [J'_F(y/x_\psi) + 2(y/x_\psi) J''_F(y/x_\psi)] Y_{1/4}^2(y) \mathcal{F}_J(y, x_\psi), \quad (42)$$

$$\mathcal{F}_{JYY}(x, x_\psi) = x_\psi \int_0^x dy [J'_F(y/x_\psi) + 2(y/x_\psi) J''_F(y/x_\psi)] J_{1/4}(y) Y_{1/4}(y) \mathcal{F}_Y(y, x_\psi). \quad (43)$$

For simplicity we have neglected the variation of g_* with temperature in (33). This allows us to obtain semi-analytic solutions in the asymptotic large and small κ limits, while only having a small numerical impact on our results.

Using the large x expansions for the Bessel functions in Eq. (33) and taking the upper integration limit $x \rightarrow \infty$ in the integrals (36-43), the unique late-time solution for the

	$x_\psi \ll 1$	$x_\psi \gg 1$
$F_J(x_\psi)$	$-4.25 x_\psi^{3/2}$	-0.338
$F_Y(x_\psi)$	$2.60 x_\psi$	$(0.0791 + 0.0429 \log x_\psi)/x_\psi$
$F_{JJ}(x_\psi)$	$7.89 x_\psi^{5/2}$	$-(0.0337 + 0.131 \log x_\psi) x_\psi$
$F_{JY}(x_\psi)$	$-2.58 x_\psi^2$	$0.206 x_\psi$
$F_{JYJ}(x_\psi)$	$7.57 x_\psi^{7/2}$	$-(0.00665 + 0.00470 \log x_\psi)$
$F_{JJY}(x_\psi)$	$18.1 x_\psi^{7/2}$	$-0.0695 x_\psi$
$F_{YYJ}(x_\psi)$	$-2.57 x_\psi^3$	$(-0.0420 + 0.0443 \log x_\psi) x_\psi$
$F_{JYY}(x_\psi)$	$-5.70 x_\psi^3$	$0.0200 x_\psi$

TABLE I. Asymptotic forms of the integrals in the small and large x_ψ regimes.

background satisfying the initial conditions can be written as

$$\varphi_0(x) \simeq \varphi_{\text{osc}} \left(\frac{x_{\text{osc}}}{x} \right)^{3/4} \sin \left(x + \frac{\pi}{8} + \theta_0 \right). \quad (44)$$

Here $x_{\text{osc}} = 3/2$ is the time corresponding to the onset of oscillations, defined by the condition $3H(x_{\text{osc}}) = m_\phi$. Furthermore, φ_{osc} and θ_0 are the effective oscillation amplitude and induced phase angle, respectively, given by

$$\varphi_{\text{osc}} = x_{\text{osc}}^{-3/4} (2/\pi)^{1/2} \sqrt{[A(x_\psi)]^2 + [B(x_\psi)]^2}, \quad \tan \theta_0 = -\frac{B(x_\psi)}{A(x_\psi)}, \quad (45)$$

where $A(x_\psi) \equiv \lim_{x \rightarrow \infty} \mathcal{A}(x, x_\psi)$, $B(x_\psi) \equiv \lim_{x \rightarrow \infty} \mathcal{B}(x, x_\psi)$ are the coefficients (34,35) in the limit $x \rightarrow \infty$. The functions $A(x_\psi)$ and $B(x_\psi)$ depend on the integrals in Eqs. (36–43) evaluated in the $x \rightarrow \infty$ limit. Thus, we define $F_J(x_\psi) \equiv \lim_{x \rightarrow \infty} \mathcal{F}_J(x, x_\psi)$, $F_Y(x_\psi) \equiv \lim_{x \rightarrow \infty} \mathcal{F}_Y(x, x_\psi)$, etc., analogously to $A(x_\psi)$ and $B(x_\psi)$. For general values of x_ψ these integrals must be evaluated numerically. However, one may also obtain asymptotic expressions for these integrals in the small x_ψ and large x_ψ regimes, which are presented in Table I. The numerical evolution of the background field φ_0 is shown in Fig. 1 in the small κ and large κ limits for thermal misalignment with $\varphi_{0i} \rightarrow 0$, along with a comparison to the standard misalignment case, $\beta \rightarrow 0$, $\varphi_{0i} \neq 0$.

The DM energy density today is given by $\rho_{\phi,0} = \frac{1}{2} m_\phi^2 M_{\text{pl}}^2 \varphi_{\text{osc}}^2 (T_0/T_{\text{osc}})^3 (g_{*S,0}/g_{*S,\text{osc}})$, where $T_0 = 2.7$ K is the CMB temperature today and $g_{*S,0} = 3.91$. The present-day DM density parameter is then given by $\Omega_\phi = \rho_{\phi,0}/\rho_{c,0}$, where $\rho_{c,0} = 3M_{\text{pl}}^2 H_0^2$ the critical density. This should be compared to the observed DM density $\Omega_{\text{DM}} = 0.26$ [1].

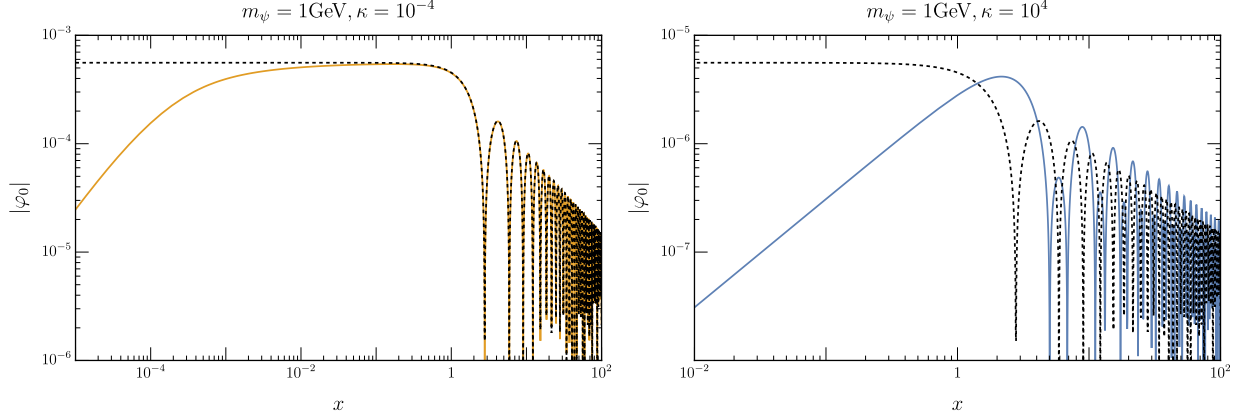


FIG. 1. Evolution of $|\varphi_0|$ in the thermal misalignment scenario with $\varphi_{0i} = 0$. The left (right) plot shows the evolution of the scalar in the small (large) κ limit where we have chosen the coupling β to reproduce the observed relic density (colored lines); see Eqs. (47,50). For comparison, we also show the evolution of scalar background in the standard misalignment scenario (black dashed lines). In the small κ limit the scalar gets misaligned at small x in the presence of the thermal potential which becomes subdominant at $x \simeq x_\psi \ll 1$. The zero mode asymptotes to a constant value and then starts to oscillate, such that at late times the oscillations are in phase with the corresponding evolution in the standard misalignment scenario ($\theta_0 \simeq 0$). At large κ , the thermal potential is dominant around the onset of oscillations and the background field is moving with a large velocity. The late time oscillations of φ_0 for large κ are out of phase with the corresponding evolution in standard misalignment with $\theta_0 \simeq -\pi/2$.

Before discussing the case of thermal misalignment, we can recover the familiar results for the case of standard misalignment by taking the limit $\beta \rightarrow 0$, in which case Eq. (45) gives the oscillation amplitude and phase, respectively, of $\varphi_{\text{osc}} \simeq 0.63 \varphi_{0i}$ and $\theta_0 = 0$. The DM relic density is then given by

$$\begin{aligned} \Omega_\phi &\simeq 0.2 \frac{g_{*S,0}^{1/4}}{g_{*,\text{osc}}} \varphi_{0i}^2 \frac{\sqrt{m_\phi M_{\text{pl}}} T_0^3}{\rho_{c,0}} \\ &\simeq 0.2 \left(\frac{\varphi_{0i}}{4 \times 10^{-5}} \right)^2 \left(\frac{m_\phi}{10^{-9} \text{ eV}} \right)^{1/2} \left(\frac{106.75}{g_{*,\text{osc}}} \right)^{1/4}. \end{aligned} \quad (46)$$

In the case of standard misalignment, we see from Eq. (46) that the DM abundance is determined by the initial field value.

Turning now to the thermal misalignment regime, we take the limit $\varphi_{0i} \rightarrow 0$ so that the misalignment is primarily dynamically generated early in the radiation era. For the purposes

of determining the relic abundance, it is enough to retain zeroth order solution $\varphi_0^{(0)}$, such that

$$\varphi_{\text{osc}} \simeq \frac{g_\psi}{(6\pi^2)^{3/4}\gamma} \frac{\beta}{\kappa} \sqrt{[F_J(x_\psi)]^2 + [F_Y(x_\psi)]^2}. \quad (47)$$

As discussed in Ref. [7], and as can be seen from Fig. 2, there are two main regions. Region 1 corresponds to $x_\psi \gg 1$, for which $F_J(x_\psi) \simeq -0.338$ dominates over $F_Y(x_\psi)$. The DM relic density in this region is

$$\begin{aligned} \Omega_\phi &\simeq 0.018 \frac{g_{*S,0}}{g_{*,\text{osc}}^{5/4}} \frac{\beta^2 m_\psi^4 T_0^3}{(m_\phi M_{\text{pl}})^{3/2} \rho_{c,0}} \\ &\simeq 0.2 \left(\frac{\beta}{0.02}\right)^2 \left(\frac{m_\psi}{1 \text{ TeV}}\right)^4 \left(\frac{1 \text{ eV}}{m_\phi}\right)^{3/2} \left(\frac{106.75}{g_{*,\text{osc}}}\right)^{5/4}, \\ &\simeq 0.2 \left(\frac{\beta}{0.01}\right)^2 \left(\frac{10^3}{\kappa}\right)^{3/2} \left(\frac{m_\psi}{1 \text{ TeV}}\right) \left(\frac{106.75}{g_{*,\text{osc}}}\right)^{5/4}. \end{aligned} \quad (48)$$

where in the first line we have written the relic density as a function of the scalar mass m_ϕ and in the second line we have replaced m_ϕ for the dimensionless mass parameter κ . Region II corresponds to $x_\psi \ll 1$, for which $F_Y(x_\psi) \simeq 2.6x_\psi$ dominates over $F_J(x_\psi)$. The DM relic density in this region is

$$\begin{aligned} \Omega_\phi &\simeq 2.4 \frac{g_{*S,0}}{g_{*,\text{osc}}^{9/4}} \frac{\beta^2 (m_\phi M_{\text{pl}})^{1/2} T_0^3}{\rho_{c,0}} \\ &\simeq 0.2 \left(\frac{\beta}{4 \times 10^{-4}}\right)^2 \left(\frac{m_\phi}{10^{-7} \text{ eV}}\right)^{1/2} \left(\frac{106.75}{g_{*,\text{osc}}}\right)^{9/4}, \\ &\simeq 0.2 \left(\frac{\beta}{5 \times 10^{-4}}\right)^2 \left(\frac{\kappa}{10^{-4}}\right)^{1/2} \left(\frac{m_\psi}{1 \text{ TeV}}\right) \left(\frac{106.75}{g_{*,\text{osc}}}\right)^{9/4}. \end{aligned} \quad (49)$$

It is useful to define the quantity φ_{DM} corresponding to the effective initial field value prior to the onset of oscillations which yields the observed DM abundance. It is given by

$$\begin{aligned} \varphi_{\text{DM}} &= \varphi_{\text{osc,DM}} \frac{3^{3/4} \sqrt{\pi}}{2^{3/2} \Gamma(5/4)} \simeq 2.2 \frac{g_{*,\text{osc}}^{1/8}}{g_{*S,0}^{1/2}} \left(\frac{\rho_{c,0} \Omega_{\text{DM}}}{T_0^3 \sqrt{m_\phi M_{\text{pl}}}}\right)^{1/2} \\ &= 2.5 \times 10^{-7} \left(\frac{g_{*,\text{osc}}}{106.75}\right)^{1/8} \left(\frac{1 \text{ eV}}{m_\phi}\right)^{1/4}, \\ &= 5.5 \times 10^{-5} \left(\frac{g_{*,\text{osc}}}{106.75}\right)^{1/8} \left(\frac{1 \text{ GeV}}{m_\psi}\right)^{1/2} \kappa^{-1/4}. \end{aligned} \quad (50)$$

Using Eqs. (50, 47), we can determine the coupling β required to generate the observed DM relic density as a function of κ for a given fermion mass, as shown in Fig. 2.

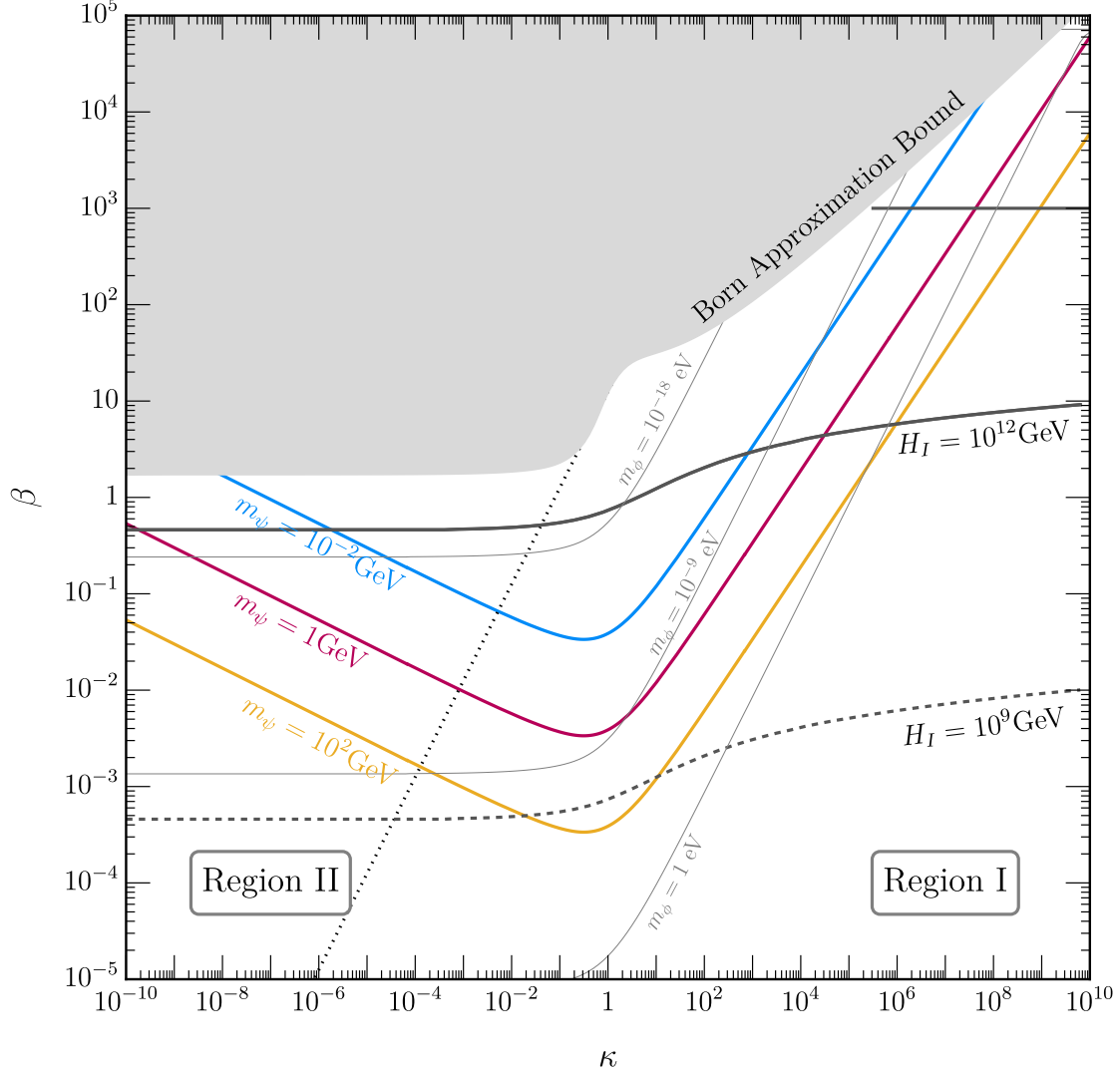


FIG. 2. *Thermal misalignment parameter space*: Solid colored contours show the values of β as a function of κ that reproduce the observed relic density for fermion masses $m_\psi = 10^{-2}$ GeV (teal), $m_\psi = 1$ GeV (magenta), $m_\psi = 10^2$ GeV (yellow). The shaded region denotes the parameter space in which the Born approximation is no longer valid (see Eq. (58)). The dotted black line indicates the approximate naturalness condition $\beta = 4\pi\kappa$, above which the radiative corrections to the zero temperature scalar potential dominate over its bare value. Thin gray lines represent isocontours of m_ϕ . The region within the solid black lines (above the dashed black line) indicate parameters consistent with the CMB isocurvature constraints for $H_I = 10^{12}$ GeV ($H_I = 10^9$ GeV). As we will show in the following sections, thermal misalignment opens up a region of $m_\phi - H_I$ parameter space for large H_I that is ruled out for standard misalignment from isocurvature bounds (see Fig. 4).

IV. EVOLUTION OF THE PERTURBATIONS

Having examined the background evolution and the DM relic abundance, we now turn to the evolution of the superhorizon scalar perturbations. Only the superhorizon evolution is relevant for our purposes, because the CMB-scale modes that constrain isocurvature remain outside the horizon during thermal misalignment. The evolution equation for the superhorizon mode $\varphi_1(x, \mathbf{k})$ (recall that $x = m_\phi t$ is the dimensionless time variable) is given in Eq. (16) together with Eqs. (20,21,22). In general, the solution for the superhorizon perturbations can be written as [32, 35, 86]³

$$\varphi_1 = f + \Psi x \frac{d\varphi_0}{dx}. \quad (51)$$

Here, the second term represents the adiabatic mode, while the first term, f , represents the isocurvature mode.

Plugging Eq. (51) into Eq. (16), we obtain the following evolution equation for f :

$$\frac{d^2 f}{dx^2} + \frac{3}{2x} \frac{df}{dx} + \mathcal{V}_{\varphi\varphi} f = 0, \quad (52)$$

where $\mathcal{V}_{\varphi\varphi}$ is defined in Eq. (21). For initial conditions at $x_i \simeq 0$ given by $f(0) = \varphi_1(0) = \varphi_{1i}$, $df(0)/dx = 0$, the solution for the isocurvature mode is given by [35]

$$\begin{aligned} f(x) &= \varphi_{1i} \frac{\partial \varphi_0(x, \varphi_{0i})}{\partial \varphi_{0i}} \\ &\simeq \varphi_{1i} 2^{1/4} \Gamma(5/4) \left[\mathcal{C}(x, x_\psi) \frac{J_{1/4}(x)}{x^{1/4}} + \mathcal{D}(x, x_\psi) \frac{Y_{1/4}(x)}{x^{1/4}} \right], \end{aligned} \quad (53)$$

where we used the solution for the background in Eq. (33). One may verify by direct substitution that Eq. (53) satisfies Eq. (52). The coefficients \mathcal{C} and \mathcal{D} are given by

$$\mathcal{C}(x, x_\psi) = 1 - \frac{g_\psi \beta^2}{2\pi \kappa^2} \mathcal{F}_{JY}(x, x_\psi), \quad (54)$$

$$\mathcal{D}(x, x_\psi) = \frac{g_\psi \beta^2}{2\pi \kappa^2} \mathcal{F}_{JJ}(x, x_\psi), \quad (55)$$

with integrals \mathcal{F}_{JJ} , \mathcal{F}_{JY} given in Eqs. (38,39)

Using the large x expansions for the Bessel functions in Eq. (53) the late-time solution for $f(x)$ can be written as

$$f(x) \simeq f_{\text{osc}} \left(\frac{x_{\text{osc}}}{x} \right)^{3/4} \sin \left(x + \frac{\pi}{8} + \theta_1 \right). \quad (56)$$

³ For brevity, we use the same notation for the Fourier-space perturbation and its mode function; the precise meaning should be apparent from the context.

Here $x_{\text{osc}} = 3/2$ is again the time corresponding to the onset of oscillations, while f_{osc} and θ_1 are the effective oscillation amplitude and induced phase angle, respectively, given by

$$f_{\text{osc}} = x_{\text{osc}}^{-3/4} \varphi_{1i} \frac{2^{3/4} \Gamma(5/4)}{\sqrt{\pi}} \sqrt{[C(x_\psi)]^2 + [D(x_\psi)]^2}, \quad \tan \theta_1 = -\frac{D(x_\psi)}{C(x_\psi)}, \quad (57)$$

where $C(x) \equiv \lim_{x \rightarrow \infty} \mathcal{C}(x, x_\psi)$, $D(x) \equiv \lim_{x \rightarrow \infty} \mathcal{D}(x, x_\psi)$ are the coefficients (54,55) in the limit $x \rightarrow \infty$.

We note that for the Born approximation to hold, the correction to the amplitude of f from the thermal effect should be small, i.e.,

$$\left| \frac{g_\psi \beta^2}{2\pi \kappa^2} F_{JJ}(x_\psi) \right|, \left| \frac{g_\psi \beta^2}{2\pi \kappa^2} F_{JY}(x_\psi) \right| \ll 1. \quad (58)$$

This condition delineates the region of validity of our analysis and is shown in Fig. 2⁴.

V. ISOCURVATURE PERTURBATIONS

With the solutions to the scalar DM background and superhorizon perturbations in hand, we can compute the superhorizon isocurvature power spectrum at late times in the radiation domination era. Precision CMB measurements from Planck and Atacama Cosmology Telescope have placed stringent constraints on the amount of DM isocurvature, which would leave distinctive imprints on the CMB power spectrum [36, 87]. By computing the effects on the superhorizon evolution for large-scale CMB modes, we can translate these isocurvature constraints to bounds on thermal misalignment parameters.

The gauge invariant isocurvature perturbation \mathcal{S} for the scalar field ϕ [78, 88, 89], is

$$\mathcal{S} = 3(\zeta_\gamma - \zeta_\phi), \quad (59)$$

where ζ_α is the curvature perturbation on uniform α -fluid density hypersurfaces [89] defined as

$$\zeta_\alpha = \Phi - H \frac{\delta\rho_\alpha}{d\rho_\alpha/dt}. \quad (60)$$

Plugging Eq. (60) into (59), we obtain

$$\mathcal{S} = 3H \left(\frac{\delta\rho_\phi}{d\rho_\phi/dt} - \frac{\delta\rho_\gamma}{d\rho_\gamma/dt} \right) = \frac{3}{2x} \left(\frac{\delta\rho_\phi}{d\rho_\phi/dx} - \Psi x \right). \quad (61)$$

⁴ A similar condition applies to corrections to the zero mode, and we have checked that it gives a numerically similar constraint.

In the second step above we have used the radiation continuity equation $d\rho_\gamma/dt = -4H\rho_\gamma$, the relation $\delta\rho_\gamma/\rho_\gamma = -2\Psi$ for superhorizon modes [76], and changed time variables to $x = m_\phi t$.

Furthermore, using Eqs. (17,18) for the background and perturbed ϕ energy densities, the ϕ continuity equation $d\rho_\phi/dx = -3/(2x)\rho_\phi$, and the solution for the superhorizon perturbation (51), we arrive at the expression

$$\mathcal{S} = -2 \frac{(d\varphi_0/dx)(df/dx) + \varphi_0 f}{(d\varphi_0/dx)^2 + \varphi_0^2}. \quad (62)$$

Finally, plugging in the late time solutions for the background and superhorizon perturbations, Eqs. (44) and (56), respectively, we obtain the compact expression

$$\mathcal{S} = -2 \frac{f_{\text{osc}}}{\varphi_{\text{osc}}} \cos(\theta_0 - \theta_1). \quad (63)$$

where the oscillation amplitudes and phase angles for the background and perturbation are given in Eqs. (45,56). We now fix the parameters by requiring agreement with the observed DM relic abundance, implying $\varphi_{\text{osc}} \simeq 0.63\varphi_{\text{DM}}$, where φ_{DM} is given in Eq. (50). Furthermore, we restrict our focus to the regime in which the Born approximation is valid such that $f_{\text{osc}} \simeq 0.63\varphi_{1i}$ (see Eqs. (57,58)) leading to the simple result

$$\mathcal{S} \simeq -2 \frac{\varphi_{1i}}{\varphi_{\text{DM}}} \cos(\theta_0 - \theta_1). \quad (64)$$

Assuming a standard slow-roll inflationary era which preceded radiation domination, characterized by Hubble parameter H_I and slow-roll parameter $\epsilon \equiv -\dot{H}_I/H_I^2 \ll 1$, and taking $m_\phi \ll H_I$, perturbations of the scalar field generated during inflation acquire a nearly scale-invariant power spectrum,

$$\mathcal{P}_{\phi_1}(k) = \frac{k^3}{2\pi^2} M_{\text{pl}}^2 |\varphi_1(\mathbf{k})|^2 \simeq \left(\frac{H_I}{2\pi} \right)^2. \quad (65)$$

These perturbations subsequently source isocurvature fluctuations during the radiation era, yielding

$$\mathcal{P}_{\mathcal{S}}(k) = \frac{k^3}{2\pi^2} |\mathcal{S}(\mathbf{k})|^2 = \frac{4}{M_{\text{pl}}^2 \varphi_{\text{DM}}^2} \cos^2(\theta_0 - \theta_1) \mathcal{P}_{\phi_1}|_i \equiv A_{\mathcal{S}} \left(\frac{k}{k_*} \right)^{n_{\mathcal{S}}-1}, \quad (66)$$

where k_* is the pivot scale. As a direct consequence of the scale invariance of \mathcal{P}_{ϕ_1} , the resulting isocurvature spectrum is also nearly scale invariant, $n_{\mathcal{S}} \simeq 1$, with amplitude

$$A_{\mathcal{S}} \equiv \frac{H_I^2}{\pi^2 M_{\text{pl}}^2 \varphi_{\text{DM}}^2} \cos^2(\theta_0 - \theta_1). \quad (67)$$

Precision measurements of the CMB by *Planck* place strong constraints on primordial isocurvature perturbations [36]. In particular, *Planck* bounds the fractional contribution of isocurvature modes to the total primordial power at the pivot scale $k_* = 0.05 \text{ Mpc}^{-1}$, finding $\beta_{\text{iso}}(k_*) < 0.038$ for uncorrelated isocurvature with a nearly scale-invariant spectrum. Using the measured scalar amplitude $A_s = 2 \times 10^{-9}$, this implies the constraint $A_{\mathcal{S}} \lesssim 0.038 A_s$, which we use throughout in constraining the parameter space of the model.

VI. RESULTS AND DISCUSSION

We now consider several limiting cases of the induced phase angles θ_0 and θ_1 , Eqs. (45,57), along with Eq. (67) to obtain approximate expressions for the final isocurvature amplitude. First we will consider the standard misalignment (sm) limit in which we set $\beta = 0$ and allow $\varphi_{0i} \neq 0$. In this limit we get $\theta_0, \theta_1 = 0$. We reproduce the well known isocurvature result (see, e.g., [33])⁵

$$A_{\mathcal{S},\text{sm}} = \frac{H_I^2}{\pi^2 M_{\text{pl}}^2 \varphi_{\text{DM}}^2}. \quad (68)$$

Imposing the isocurvature constraint $A_{\mathcal{S}} \lesssim 0.038 A_s$ we obtain an upper bound on H_I given by

$$H_I \leq 1.7 \times 10^7 \text{ GeV} \left(\frac{1 \text{ eV}}{m_\phi} \right)^{1/4} \left(\frac{g_{*,\text{osc}}}{106.75} \right)^{1/8}. \quad (69)$$

The resulting limit is shown in Fig. 4.

Next we consider the thermal misalignment (tm) limit in which $\varphi_{0i} = 0$ and $\beta \neq 0$. The induced phase angles associated with the zero mode and superhorizon perturbations can be written as

$$\theta_0 = -\tan^{-1} \left(\frac{B(x_\psi)}{A(x_\psi)} \right) = \tan^{-1} \left(\frac{F_J(x_\psi) + \frac{g_\psi \beta^2}{2\pi \kappa^2} [F_{JYJ}(x_\psi) - F_{JJY}(x_\psi)]}{F_Y(x_\psi) + \frac{g_\psi \beta^2}{2\pi \kappa^2} [F_{YYJ}(x_\psi) - F_{JYY}(x_\psi)]} \right), \quad (70)$$

$$\theta_1 = -\tan^{-1} \left(\frac{D(x_\psi)}{C(x_\psi)} \right) = -\tan^{-1} \left(\frac{\frac{g_\psi \beta^2}{2\pi \kappa^2} F_{JJ}(x_\psi)}{1 - \frac{g_\psi \beta^2}{2\pi \kappa^2} F_{JY}(x_\psi)} \right) \simeq -\frac{g_\psi \beta^2}{2\pi \kappa^2} F_{JJ}(x_\psi). \quad (71)$$

In the last expression for θ_1 we have restricted to the domain where the Born approximation, Eq. (58), is valid. We also note that $\theta_1 \ll 1$ throughout this regime, i.e., the phase of the superhorizon perturbations is similar in standard and thermal misalignment.

⁵ The same well-known result is obtained for QCD axion DM up to anharmonic corrections [23–28, 32]

To further understand the behavior of isocurvature perturbations in thermal misalignment, we examine the two regimes $\kappa \ll 1$ ($x_\psi \ll 1$) and $\kappa \gg 1$ ($x_\psi \gg 1$). Taking first the small κ (small x_ψ) limit, Region 2, we make use of the asymptotic forms of the integrals given in Table I and fix the coupling β to match the observed DM relic using Eqs. (47,50), obtaining

$$\theta_0 \simeq \frac{F_J(x_\psi)}{F_Y(x_\psi)} \simeq -1.63x_\psi^{1/2}, \quad (72)$$

$$\theta_1 \simeq -10^{-9} \left(\frac{100 \text{ GeV}}{m_\psi} \right) \left(\frac{g_{*,\text{osc}}}{106.75} \right) \frac{F_{JJ}(x_\psi)}{x_\psi^{1/2} [F_Y(x_\psi)]^2} \simeq -10^{-9} \left(\frac{100 \text{ GeV}}{m_\psi} \right) \left(\frac{g_{*,\text{osc}}}{106.75} \right). \quad (73)$$

Both of the induced phase angles θ_0 and θ_1 are parametrically small, implying that $\cos(\theta_0 - \theta_1) \simeq 1$. Therefore, for small κ the isocurvature amplitude in thermal misalignment coincides with the standard misalignment result, Eq. (68). This can also be understood from Fig. 1 which shows that the phase of the late-time zero mode oscillations in thermal misalignment is nearly identical to that in standard misalignment.

The $\kappa \gg 1$ ($x_\psi \gg 1$) limit, Region 1, exhibits more interesting behavior. Again making use of the asymptotic forms of the integrals presented in Table I and setting the coupling β to reproduce the correct relic abundance using Eqs. (47,50), we obtain

$$\theta_0 = -\tan^{-1} \left(\frac{B(x_\psi)}{A(x_\psi)} \right) \simeq -\frac{\pi}{2} + \frac{A(x_\psi)}{B(x_\psi)} \quad (74)$$

$$\simeq -\frac{\pi}{2} - \frac{F_Y(x_\psi) + \frac{g_\psi}{2\pi} \frac{\beta^2}{\kappa^2} [F_{YYJ}(x_\psi) - F_{JYY}(x_\psi)]}{F_J(x_\psi)}$$

$$\simeq -\frac{\pi}{2} + \frac{(0.234 + 0.127 \log x_\psi)}{x_\psi} + 10^{-9} \left(\frac{100 \text{ GeV}}{m_\psi} \right) \left(\frac{g_{*,\text{osc}}}{106.75} \right) (-1.61 + 1.15 \log x_\psi) x_\psi^{1/2},$$

$$\theta_1 \simeq -10^{-9} \left(\frac{100 \text{ GeV}}{m_\psi} \right) \left(\frac{g_{*,\text{osc}}}{106.75} \right) \frac{F_{JJ}(x_\psi)}{x_\psi^{1/2} [F_J(x_\psi)]^2} \quad (75)$$

$$\simeq -10^{-9} \left(\frac{100 \text{ GeV}}{m_\psi} \right) \left(\frac{g_{*,\text{osc}}}{106.75} \right) (0.296 + 1.15 \log x_\psi) x_\psi^{1/2}.$$

For $\kappa \gg 1$ ($x_\psi \gg 1$), the thermal potential is unsuppressed at the onset of oscillations ($3H = m_\phi, x_{\text{osc}} = 3/2$). As a result, the zero mode is generically not released from rest as in standard misalignment, but rather has a substantial velocity at x_{osc} . This results in a late-time oscillatory solution with a phase that is shifted by approximately $-\pi/2$ relative to the standard misalignment solution, which is captured by the leading term $\theta_0 \simeq -\pi/2$ in Eq. (74). The remaining terms in θ_0 and θ_1 are subleading corrections, controlled by the

large- x_ψ asymptotics and by restricting to the parameter space where the Born approximation is valid. In particular, imposing the Born-validity condition in Eq. (58) ensures these corrections remain small, i.e., $|\theta_0 + \pi/2| \ll 1$ and $|\theta_1| \ll 1$.

Using these results, the isocurvature amplitude for $\kappa \gg 1$ may be written as

$$\begin{aligned}
A_{\mathcal{S},\text{tm}} &\simeq A_{\mathcal{S},\text{sm}} \times \left[-\frac{F_Y(x_\psi)}{F_J(x_\psi)} - \frac{g_\psi \beta^2}{2\pi \kappa^2} \left(\frac{[F_{YYJ}(x_\psi) - F_{JYY}(x_\psi)]}{F_J(x_\psi)} - F_{JJ}(x_\psi) \right) \right]^2 \\
&= A_{\mathcal{S},\text{sm}} \times \left[\frac{(0.234 + 0.127 \log x_\psi)}{x_\psi} - 1.90 \times 10^{-9} \left(\frac{100 \text{ GeV}}{m_\psi} \right) \left(\frac{g_{*,\text{osc}}}{106.75} \right) x_\psi^{1/2} \right]^2.
\end{aligned} \tag{76}$$

The factor in brackets in Eq. (76) controls the ratio of isocurvature amplitudes, $\sqrt{|A_{\mathcal{S},\text{tm}}/A_{\mathcal{S},\text{sm}}|} \simeq |\cos(\theta_0 - \theta_1)|$. For intermediate $x_\psi \gg 1$, the first term $\sim (c_1 + c_2 \log x_\psi)/x_\psi$ dominates, so the ratio $\sqrt{|A_{\mathcal{S},\text{tm}}/A_{\mathcal{S},\text{sm}}|}$ decreases with increasing x_ψ and the isocurvature amplitude is increasingly suppressed. At larger x_ψ , the second term grows as $x_\psi^{1/2}$, leading to a value $x_\psi = \hat{x}_\psi$ where the bracketed term vanishes and hence $A_{\mathcal{S},\text{tm}} \rightarrow 0$, given approximately by

$$\begin{aligned}
\hat{x}_\psi &\simeq 1.26 \times 10^5 \left(\frac{m_\psi}{100 \text{ GeV}} \right)^{2/3} \left(\frac{106.75}{g_{*,\text{osc}}} \right)^{2/3} \left\{ 20.4 + \log \left[\left(\frac{m_\psi}{100 \text{ GeV}} \right) \left(\frac{106.75}{g_{*,\text{osc}}} \right) \right] \right. \\
&\quad \left. + \log \left[20.4 + \log \left[\left(\frac{m_\psi}{100 \text{ GeV}} \right) \left(\frac{106.75}{g_{*,\text{osc}}} \right) \right] \right] \right\}^{2/3}.
\end{aligned} \tag{77}$$

Physically, this corresponds to a relative induced phase between the zero mode and its perturbation that yields complete cancellation of the isocurvature amplitude. For even larger x_ψ , the $x_\psi^{1/2}$ term dominates and $\mathcal{S}_{\text{ratio}}$ increases until the Born-validity bound in Eq. (58) is reached. This behavior, including the single zero crossing, is shown in Fig. 3. We have numerically verified our analytical results for several benchmarks.

The suppression of isocurvature relative to standard misalignment permits larger values of H_I without running afoul of observational isocurvature bounds. This enlarges the viable parameter space, making light scalar DM compatible with high-scale inflation. Since the isocurvature bound is appreciably relaxed only for $\kappa \equiv m_\phi M_{\text{pl}}/m_\psi^2 \gg 1$, the impacted range of scalar masses depends on the fermion mass m_ψ . Fig. 4 illustrates the resulting enlargement of viable parameter space for several representative choices of fermion masses.

The above result was derived in the limit $\varphi_{0i} = 0$. However, for a small but finite $\varphi_{0i} \ll \varphi_{\text{DM}}$, the suppression factor in the brackets of Eq. (76) receives an additional contribution of $\varphi_{0i}/\varphi_{\text{DM}}$, setting a floor on the extent to which isocurvature can be suppressed.

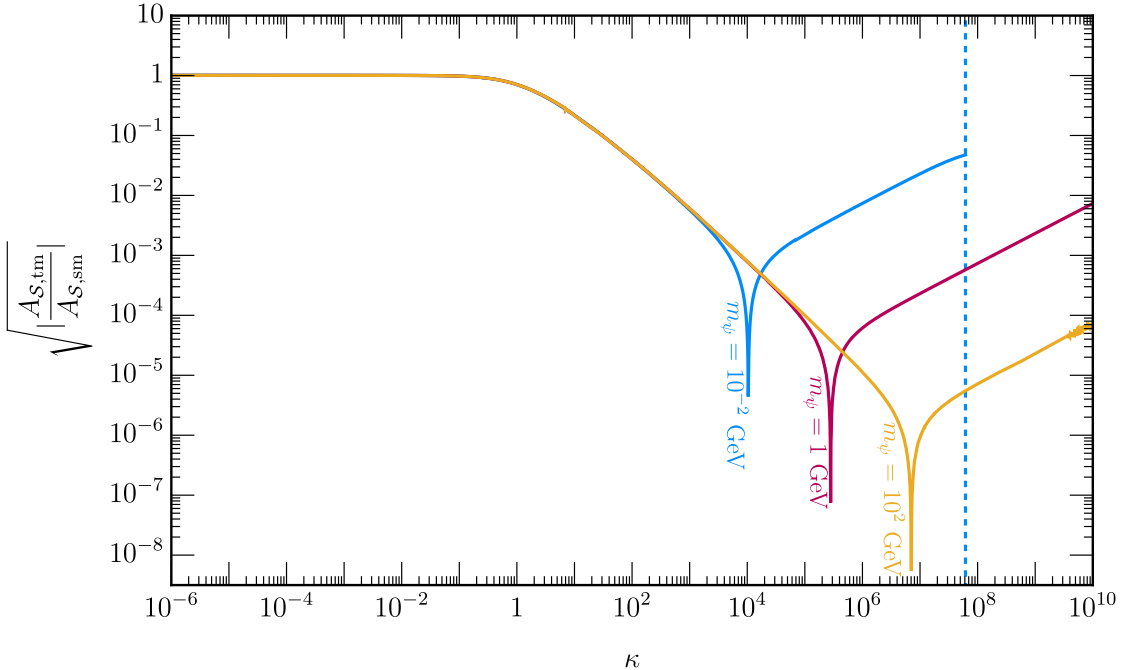


FIG. 3. Square root of the isocurvature amplitude ratio between thermal misalignment and standard misalignment, $\sqrt{|A_{S,tm}/A_{S,sm}|}$ obtained using using Eqs. (67, 68). We have chosen three representative fermion masses, $m_\psi = 10^2$ GeV (yellow), 1 GeV (magenta), 10^{-2} GeV (blue). For $m_\psi = 10^{-2}$ GeV the vertical dashed line indicates the values of κ above which the Born approximation fails (see Eq. (58)). The isocurvature in thermal misalignment exhibits the expected cosine dependence, with the amplitude ratio decreasing to zero before rising again. We can see the cosine behavior for isocurvature in thermal misalignment, as magnitude isocurvature ratio decreases to be exactly zero and increases again.

VII. OUTLOOK

In this work we have studied the generation of DM isocurvature perturbations in the framework of thermal misalignment. We showed that, unlike in standard misalignment, the isocurvature signal can be naturally suppressed in regions of parameter space where the scalar begins oscillating while the thermal potential still dominates. Physically, this suppression arises because the thermal potential gives the zero mode a nonzero initial velocity at the onset of oscillations, producing a late-time phase offset relative to the superhorizon perturbations and thereby reducing the final DM density contrast. Thermal misalignment therefore opens new parameter space for light scalar DM consistent with CMB isocurvature

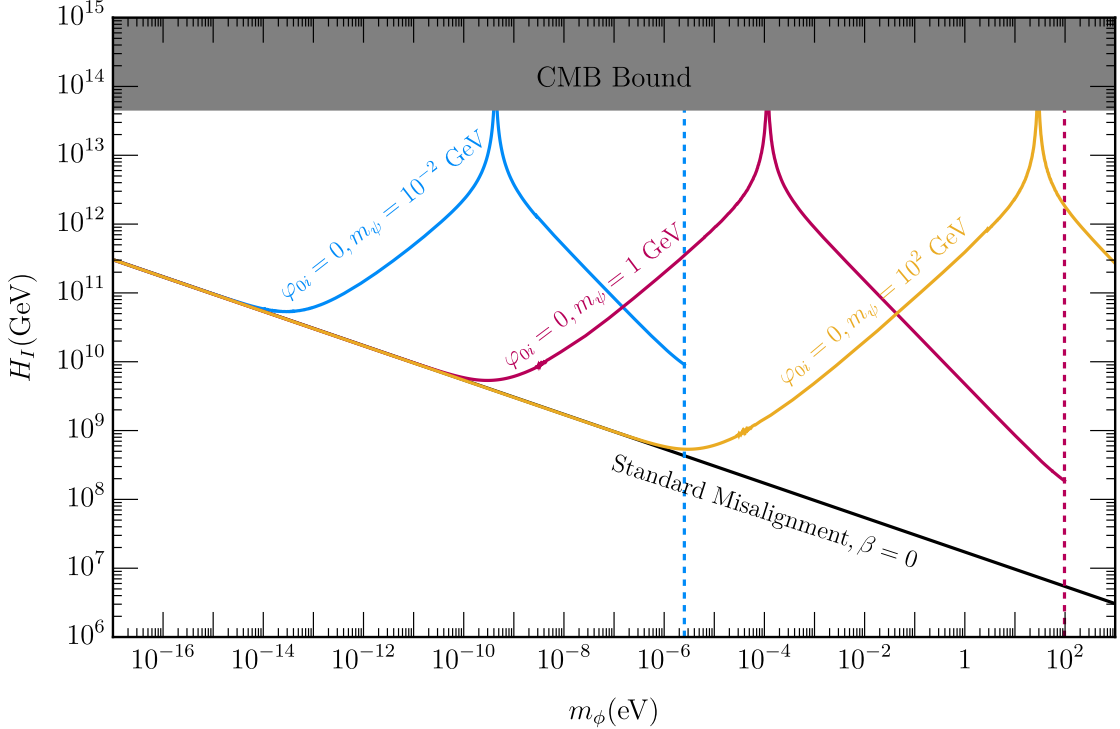


FIG. 4. The upper bound on H_I as a function of m_ϕ in thermal misalignment for several choices of fermion masses, $m_\psi = 10^2$ GeV (yellow), 1 GeV (magenta) and 10^{-2} GeV (blue), and for standard misalignment (black). For thermal misalignment, the upper bound is relaxed relative to standard misalignment over a broad scalar-mass range, with the precise interval depending on m_ψ . Vertical dashed lines indicate where the Born approximation fails (Eq. (58)). The gray band indicates the Planck + BICEP upper bound $H_I \leq 4.7 \times 10^{13}$ GeV [37] from the non-observation of CMB B-modes associated with tensor fluctuations produced during inflation.

bounds and with well-motivated models of high-scale inflation.

There are several directions that deserve further study. The thermal potential induces energy and momentum exchange between ϕ and the thermal bath, modifying the evolution of both adiabatic and isocurvature perturbations. In this language, the isocurvature suppression found here can be understood as a consequence of energy and momentum transfer between the two sectors [78, 90–94], a perspective that we plan to develop further in future work [95]. It would also be interesting to study the impact of thermal misalignment on the matter power spectrum at large k . One further direction is to explore other mechanisms beyond thermal misalignment which realize the phase off-set between the zero mode and superhorizon perturbations as a means to suppress DM isocurvature.

Finally, while we have focused here on a minimal realization involving a scalar interacting with a bath fermion via a Yukawa coupling, it would be valuable to extend the analysis to a broader class of models. Particularly interesting are scenarios in which scalar DM has shift-symmetry-breaking couplings to SM particles, potentially leading to additional experimental signatures that could test the relic-density prediction of thermal misalignment.

ACKNOWLEDGMENTS

We would like to thank Priyesh Chakraborty, Chandrika Chandrashekhar, Wayne Hu, Soubhik Kumar, Rashmish Mishra, Sonia Paban, Matthew Reece and Sarunas Verner for helpful conversations. The work of BB is supported by the U.S. Department of Energy under Grant No. DE-SC0007914. The work of AG is supported by the GRASP initiative at Harvard University. SG acknowledges support from the National Science Foundation (NSF) under Grant No. PHY-2413016. The work of MR is supported in part by the U.S. Department of Energy under Grant No. DE-SC0010813.

-
- [1] PLANCK collaboration, *Planck 2018 results. VI. Cosmological parameters*, *Astron. Astrophys.* **641** (2020) A6 [1807.06209].
 - [2] J. Preskill, M.B. Wise and F. Wilczek, *Cosmology of the Invisible Axion*, *Phys. Lett. B* **120** (1983) 127.
 - [3] L.F. Abbott and P. Sikivie, *A Cosmological Bound on the Invisible Axion*, *Phys. Lett. B* **120** (1983) 133.
 - [4] M. Dine and W. Fischler, *The Not So Harmless Axion*, *Phys. Lett. B* **120** (1983) 137.
 - [5] D. Antypas et al., *New Horizons: Scalar and Vector Ultralight Dark Matter*, 2203.14915.
 - [6] F. Piazza and M. Pospelov, *Sub-eV scalar dark matter through the super-renormalizable Higgs portal*, *Phys. Rev. D* **82** (2010) 043533 [1003.2313].
 - [7] B. Batell and A. Ghalsasi, *Thermal misalignment of scalar dark matter*, *Phys. Rev. D* **107** (2023) L091701 [2109.04476].
 - [8] B. Batell, A. Ghalsasi and M. Rai, *Dynamics of dark matter misalignment through the Higgs portal*, *JHEP* **01** (2024) 038 [2211.09132].

- [9] R. Fardon, A.E. Nelson and N. Weiner, *Dark energy from mass varying neutrinos*, *JCAP* **10** (2004) 005 [[astro-ph/0309800](#)].
- [10] D. Brzemiński, Z. Chacko, A. Dev and A. Hook, *Time-varying fine structure constant from naturally ultralight dark matter*, *Phys. Rev. D* **104** (2021) 075019 [[2012.02787](#)].
- [11] E.J. Chun, *Bosonic dark matter in a coherent state driven by thermal fermions*, *Phys. Lett. B* **825** (2022) 136880 [[2109.07423](#)].
- [12] C. Murgui and R. Plestid, *Coleman-Weinberg dynamics of ultralight scalar dark matter and GeV-scale right-handed neutrinos*, *JHEP* **08** (2024) 168 [[2306.13799](#)].
- [13] R. Plestid and S. Tevosyan, *The cosmology of ultralight scalar dark matter coupled to right-handed neutrinos*, *JHEP* **07** (2025) 012 [[2409.17396](#)].
- [14] D. Cyncynates and O. Simon, *Scalar Relics from the Hot Big Bang*, *Phys. Rev. Lett.* **135** (2025) 101003 [[2410.22409](#)].
- [15] D. Cyncynates and O. Simon, *Minimal targets for dilaton direct detection*, *Phys. Rev. D* **112** (2025) 055002 [[2408.16816](#)].
- [16] W. Buchmüller, K. Hamaguchi and M. Ratz, *Gauge couplings at high temperature and the relic gravitino abundance*, *Phys. Lett. B* **574** (2003) 156 [[hep-ph/0307181](#)].
- [17] W. Buchmüller, K. Hamaguchi, O. Lebedev and M. Ratz, *Dilaton destabilization at high temperature*, *Nucl. Phys. B* **699** (2004) 292 [[hep-th/0404168](#)].
- [18] T. Moroi, K. Mukaida, K. Nakayama and M. Takimoto, *Scalar Trapping and Saxion Cosmology*, *JHEP* **06** (2013) 040 [[1304.6597](#)].
- [19] B. Lillard, M. Ratz, T. Tait, M. P. and S. Trojanowski, *The Flavor of Cosmology*, *JCAP* **07** (2018) 056 [[1804.03662](#)].
- [20] D. Croon, H. Davoudiasl and R. Houtz, *Leptogenesis enabled by dark matter*, *Phys. Rev. D* **106** (2022) 035006 [[2204.07584](#)].
- [21] A. Cheek, J.K. Osiński, L. Roszkowski and S. Trojanowski, *Dark matter production through a non-thermal flavon portal*, *JHEP* **03** (2023) 149 [[2211.02057](#)].
- [22] V. Knapp-Perez, G. Mohlabeng, M. Ratz and T.M.P. Tait, *Thermal history of non-equilibrated scalars*, *JCAP* **03** (2026) 002 [[2507.21523](#)].
- [23] D. Seckel and M.S. Turner, *Isothermal Density Perturbations in an Axion Dominated Inflationary Universe*, *Phys. Rev. D* **32** (1985) 3178.
- [24] A.D. Linde, *Inflation and Axion Cosmology*, *Phys. Lett. B* **201** (1988) 437.

- [25] D.H. Lyth, *A Limit on the Inflationary Energy Density From Axion Isocurvature Fluctuations*, *Phys. Lett. B* **236** (1990) 408.
- [26] M.S. Turner and F. Wilczek, *Inflationary Axion Cosmology*, *Phys. Rev. Lett.* **66** (1991) 5.
- [27] D.H. Lyth and E.D. Stewart, *Constraining the inflationary energy scale from axion cosmology*, *Phys. Lett. B* **283** (1992) 189.
- [28] P. Fox, A. Pierce and S.D. Thomas, *Probing a QCD string axion with precision cosmological measurements*, [hep-th/0409059](#).
- [29] M.P. Hertzberg, M. Tegmark and F. Wilczek, *Axion Cosmology and the Energy Scale of Inflation*, *Phys. Rev. D* **78** (2008) 083507 [[0807.1726](#)].
- [30] D. Langlois, *Lectures on inflation and cosmological perturbations*, *Lect. Notes Phys.* **800** (2010) 1 [[1001.5259](#)].
- [31] D. Langlois and F. Vernizzi, *Mixed inflaton and curvaton perturbations*, *Phys. Rev. D* **70** (2004) 063522 [[astro-ph/0403258](#)].
- [32] T. Kobayashi, R. Kurematsu and F. Takahashi, *Isocurvature Constraints and Anharmonic Effects on QCD Axion Dark Matter*, *JCAP* **09** (2013) 032 [[1304.0922](#)].
- [33] T. Tenkanen, *Dark matter from scalar field fluctuations*, *Phys. Rev. Lett.* **123** (2019) 061302 [[1905.01214](#)].
- [34] S. Kalia, *Dynamically generated tilt of isocurvature fluctuations*, [2510.11803](#).
- [35] I.J. Allali, P. Chakraborty, J. Fan and M. Reece, *Axion Perturbations: A General Analytical Treatment*, [2510.07371](#).
- [36] PLANCK collaboration, *Planck 2018 results. X. Constraints on inflation*, *Astron. Astrophys.* **641** (2020) A10 [[1807.06211](#)].
- [37] BICEP, KECK collaboration, *Improved Constraints on Primordial Gravitational Waves using Planck, WMAP, and BICEP/Keck Observations through the 2018 Observing Season*, *Phys. Rev. Lett.* **127** (2021) 151301 [[2110.00483](#)].
- [38] K. Clough, E.A. Lim, B.S. DiNunno, W. Fischler, R. Flauger and S. Paban, *Robustness of Inflation to Inhomogeneous Initial Conditions*, *JCAP* **09** (2017) 025 [[1608.04408](#)].
- [39] M. Kawasaki and T. Yanagida, *Are isocurvature fluctuations of the M theory axion observable?*, *Prog. Theor. Phys.* **97** (1997) 809 [[hep-ph/9703261](#)].
- [40] M. Beltran, J. Garcia-Bellido and J. Lesgourgues, *Isocurvature bounds on axions revisited*, *Phys. Rev. D* **75** (2007) 103507 [[hep-ph/0606107](#)].

- [41] M. Kawasaki and T. Sekiguchi, *Cosmological Constraints on Isocurvature and Tensor Perturbations*, *Prog. Theor. Phys.* **120** (2008) 995 [0705.2853].
- [42] K.J. Mack, *Axions, Inflation and the Anthropic Principle*, *JCAP* **07** (2011) 021 [0911.0421].
- [43] P. Chakraborty, J. Cheng, M. Reece and Z. Wang, *A Step in Flux to Suppress Axion Isocurvature*, 2507.12519.
- [44] G.R. Dvali, *Removing the cosmological bound on the axion scale*, hep-ph/9505253.
- [45] K.S. Jeong and F. Takahashi, *Suppressing Isocurvature Perturbations of QCD Axion Dark Matter*, *Phys. Lett. B* **727** (2013) 448 [1304.8131].
- [46] K. Choi, E.J. Chun, S.H. Im and K.S. Jeong, *Diluting the inflationary axion fluctuation by a stronger QCD in the early Universe*, *Phys. Lett. B* **750** (2015) 26 [1505.00306].
- [47] R.T. Co, E. Gonzalez and K. Harigaya, *Axion Misalignment Driven to the Bottom*, *JHEP* **05** (2019) 162 [1812.11186].
- [48] L. Heurtier, F. Huang and T.M.P. Tait, *Resurrecting low-mass axion dark matter via a dynamical QCD scale*, *JHEP* **12** (2021) 216 [2104.13390].
- [49] M. Dine and A. Anisimov, *Is there a Peccei-Quinn phase transition?*, *JCAP* **07** (2005) 009 [hep-ph/0405256].
- [50] T. Higaki, K.S. Jeong and F. Takahashi, *Solving the Tension between High-Scale Inflation and Axion Isocurvature Perturbations*, *Phys. Lett. B* **734** (2014) 21 [1403.4186].
- [51] M. Dine and L. Stephenson-Haskins, *Hybrid Inflation with Planck Scale Fields*, *JHEP* **09** (2015) 208 [1408.0046].
- [52] M. Kawasaki, M. Yamada and T.T. Yanagida, *Cosmologically safe QCD axion as a present from extra dimension*, *Phys. Lett. B* **750** (2015) 12 [1506.05214].
- [53] F. Takahashi and M. Yamada, *Strongly broken Peccei-Quinn symmetry in the early Universe*, *JCAP* **10** (2015) 010 [1507.06387].
- [54] J. Kearney, N. Orlofsky and A. Pierce, *High-Scale Axions without Isocurvature from Inflationary Dynamics*, *Phys. Rev. D* **93** (2016) 095026 [1601.03049].
- [55] M.A. Buen-Abad and J. Fan, *Dynamical axion misalignment with small instantons*, *JHEP* **12** (2019) 161 [1911.05737].
- [56] M. Kawasaki, F. Takahashi and M. Yamada, *Suppressing the QCD Axion Abundance by Hidden Monopoles*, *Phys. Lett. B* **753** (2016) 677 [1511.05030].

- [57] Y. Nomura, S. Rajendran and F. Sanches, *Axion Isocurvature and Magnetic Monopoles*, *Phys. Rev. Lett.* **116** (2016) 141803 [1511.06347].
- [58] M. Kawasaki, F. Takahashi and M. Yamada, *Adiabatic suppression of the axion abundance and isocurvature due to coupling to hidden monopoles*, *JHEP* **01** (2018) 053 [1708.06047].
- [59] W. Fischler and J. Preskill, *DYON - AXION DYNAMICS*, *Phys. Lett. B* **125** (1983) 165.
- [60] A.D. Linde, *Axions in inflationary cosmology*, *Phys. Lett. B* **259** (1991) 38.
- [61] S. Kasuya, M. Kawasaki and T. Yanagida, *Cosmological axion problem in chaotic inflationary universe*, *Phys. Lett. B* **409** (1997) 94 [hep-ph/9608405].
- [62] S. Kasuya, M. Kawasaki and T. Yanagida, *Domain wall problem of axion and isocurvature fluctuations in chaotic inflation models*, *Phys. Lett. B* **415** (1997) 117 [hep-ph/9709202].
- [63] S. Folkerts, C. Germani and J. Redondo, *Axion Dark Matter and Planck favor non-minimal couplings to gravity*, *Phys. Lett. B* **728** (2014) 532 [1304.7270].
- [64] M. Kawasaki, T.T. Yanagida and K. Yoshino, *Domain wall and isocurvature perturbation problems in axion models*, *JCAP* **11** (2013) 030 [1305.5338].
- [65] E.J. Chun, *Axion Dark Matter with High-Scale Inflation*, *Phys. Lett. B* **735** (2014) 164 [1404.4284].
- [66] M. Fairbairn, R. Hogan and D.J.E. Marsh, *Unifying inflation and dark matter with the Peccei-Quinn field: observable axions and observable tensors*, *Phys. Rev. D* **91** (2015) 023509 [1410.1752].
- [67] K. Nakayama and M. Takimoto, *Higgs inflation and suppression of axion isocurvature perturbation*, *Phys. Lett. B* **748** (2015) 108 [1505.02119].
- [68] K. Harigaya, M. Ibe, M. Kawasaki and T.T. Yanagida, *Dynamics of Peccei-Quinn Breaking Field after Inflation and Axion Isocurvature Perturbations*, *JCAP* **11** (2015) 003 [1507.00119].
- [69] T. Kobayashi and F. Takahashi, *Cosmological Perturbations of Axion with a Dynamical Decay Constant*, *JCAP* **08** (2016) 056 [1607.04294].
- [70] I.J. Allali, M.P. Hertzberg and Y. Lyu, *Altered axion abundance from a dynamical Peccei-Quinn scale*, *Phys. Rev. D* **105** (2022) 123517 [2203.15817].
- [71] P.W. Graham and A. Scherlis, *Stochastic axion scenario*, *Phys. Rev. D* **98** (2018) 035017 [1805.07362].

- [72] J.P. Conlon and F. Revello, *Catch-me-if-you-can: the overshoot problem and the weak/inflation hierarchy*, *JHEP* **11** (2022) 155 [2207.00567].
- [73] R.T. Co, L.J. Hall and K. Harigaya, *Axion Kinetic Misalignment Mechanism*, *Phys. Rev. Lett.* **124** (2020) 251802 [1910.14152].
- [74] H. Kodama and M. Sasaki, *Cosmological Perturbation Theory*, *Prog. Theor. Phys. Suppl.* **78** (1984) 1.
- [75] V.F. Mukhanov, H.A. Feldman and R.H. Brandenberger, *Theory of cosmological perturbations. Part 1. Classical perturbations. Part 2. Quantum theory of perturbations. Part 3. Extensions*, *Phys. Rept.* **215** (1992) 203.
- [76] C.-P. Ma and E. Bertschinger, *Cosmological perturbation theory in the synchronous and conformal Newtonian gauges*, *Astrophys. J.* **455** (1995) 7 [astro-ph/9506072].
- [77] W. Hu, *Covariant linear perturbation formalism*, *ICTP Lect. Notes Ser.* **14** (2003) 145 [astro-ph/0402060].
- [78] K.A. Malik, D. Wands and C. Ungarelli, *Large scale curvature and entropy perturbations for multiple interacting fluids*, *Phys. Rev. D* **67** (2003) 063516 [astro-ph/0211602].
- [79] A.A. Starobinsky and J. Yokoyama, *Equilibrium state of a selfinteracting scalar field in the De Sitter background*, *Phys. Rev. D* **50** (1994) 6357 [astro-ph/9407016].
- [80] F. Takahashi, W. Yin and A.H. Guth, *QCD axion window and low-scale inflation*, *Phys. Rev. D* **98** (2018) 015042 [1805.08763].
- [81] S.R. Coleman and E.J. Weinberg, *Radiative Corrections as the Origin of Spontaneous Symmetry Breaking*, *Phys. Rev. D* **7** (1973) 1888.
- [82] A. Hook, *Solving the Hierarchy Problem Discretely*, *Phys. Rev. Lett.* **120** (2018) 261802 [1802.10093].
- [83] N. Herring and D. Boyanovsky, *Misalignment dynamics of scalar condensates with Yukawa coupling: Particle and entropy production*, *Phys. Rev. D* **113** (2026) 043503 [2511.22465].
- [84] J. Yokoyama and A.D. Linde, *Is warm inflation possible?*, *Phys. Rev. D* **60** (1999) 083509 [hep-ph/9809409].
- [85] A. Banerjee, N.H. Nguyen and E.H. Tanin, *Thermal Damping of Mass-Modulating Scalars*, 2512.05188.
- [86] S. Weinberg, *Adiabatic modes in cosmology*, *Phys. Rev. D* **67** (2003) 123504 [astro-ph/0302326].

- [87] ATACAMA COSMOLOGY TELESCOPE collaboration, *The Atacama Cosmology Telescope: DR6 constraints on extended cosmological models*, *JCAP* **11** (2025) 063 [2503.14454].
- [88] J.M. Bardeen, P.J. Steinhardt and M.S. Turner, *Spontaneous Creation of Almost Scale - Free Density Perturbations in an Inflationary Universe*, *Phys. Rev. D* **28** (1983) 679.
- [89] D. Wands, K.A. Malik, D.H. Lyth and A.R. Liddle, *A New approach to the evolution of cosmological perturbations on large scales*, *Phys. Rev. D* **62** (2000) 043527 [astro-ph/0003278].
- [90] S. Gupta, K.A. Malik and D. Wands, *Curvature and isocurvature perturbations in a three-fluid model of curvaton decay*, *Phys. Rev. D* **69** (2004) 063513 [astro-ph/0311562].
- [91] K.A. Malik and D. Wands, *Adiabatic and entropy perturbations with interacting fluids and fields*, *JCAP* **02** (2005) 007 [astro-ph/0411703].
- [92] N. Bellomo, K.V. Berghaus and K.K. Boddy, *Impact of freeze-in on dark matter isocurvature*, *JCAP* **11** (2023) 024 [2210.15691].
- [93] D. Racco and A. Riotto, *Freeze-in dark matter perturbations are adiabatic*, *Journal of Cosmology and Astroparticle Physics* **2023** (2023) 020.
- [94] A. Strumia, *Dark Matter from freeze-in and its inhomogeneities*, *JHEP* **03** (2023) 042 [2211.08359].
- [95] B. Batell, A. Ghalsasi, S. Ghosh and M. Rai, *in preparation*, .